Published in final edited form as:
Oncogene. 2012 July 26; 31(30): 3561–3568. doi:10.1038/onc.2011.509.

Mice deficient in MIM expression are predisposed to lymphomagenesis

Dan Yu[*], **Xiaoguo H. Zhan**[*], **Xianfeng Frank Zhao**[†], **Mark S. Williams**[*,‡], **Gregory B. Carey**[*,‡], **Elizabeth Smith**[*], **David Scott**[§], **Jianwei Zhu**[¶], **Yin Guo**[‖], **Srujana Cherukuri**[‖], **Curt I. Civin**[‖], and **Xi Zhan**[*,†,**]

[*]Center for Vascular and Inflammatory Diseases

[†]Department of Pathology

[‡]Department of Microbiology and Immunology

[§]Research Department of Medicine Uniformed Services, University of Health Sciences

[¶]Department of General Surgery, the Affiliated Hospital, Nantong University, China

[‖]Center for Stem Cell Biology & Regenerative Medicine, Department of Pediatrics and Physiology

[**]The Marlene Stewart Greenebaum Cancer Center, University of Maryland School of Medicine, Baltimore, MD 21201

Abstract

Missing in metastasis (MIM) is a member of newly emerged inverse BAR-domain protein family and a putative metastasis suppressor. Although reduced MIM expression has been associated with bladder, breast, gastric cancers, evidence for the role of MIM in tumor progression remains scarce and controversial. Herein we characterized a MIM knockout mouse strain and observed that MIM deficient mice often developed enlarged spleens. Autopsy and histological analysis revealed that nearly 78% of MIM(−/−) mice developed tumors with features similar to diffuse large B lymphoma during a period from one to two years. MIM(−/−) mice also exhibited abnormal distribution of B cells in lymphoid organs with decrease in the spleen but increase in the bone marrow and the peripheral blood. Furthermore, the bone marrow of MIM(−/−) mice contained a higher percentage of pre-B2 cells but fewer immature B-cells than wild type mice. In response to CXCL13, a B-cell chemokine released from splenic stromal cells, MIM deficient B-cells did not undergo chemotaxis or morphologic changes in response to the chemokine and also did not internalize CXCR5, the receptor of CXCL13. Microarray analyses demonstrated that MIM is the only member of the I-BAR domain family that was highly expressed in human B cells. However, low or absent MIM expression was common in either primary B-cell malignancies or established B-cell acute lymphocytic leukemia or lymphomas. Thus, our data demonstrate for the first time an important role for MIM in B-cell development and suggests that predisposition of MIM null mice to lymphomagenesis may involve aberrant interactions between B lineage cells and the lymphoid microenvironment.

Corresponding author: Xi Zhan, The Center for Vascular and Inflammatory Diseases, University of Maryland School of Medicine, 800 West Baltimore Street, MD 21201, xzhan@som.umaryland.edu, Phone: 410-706-8228.

Conflict of Interests

The authors declare no conflict of interest.

Introduction

Metastasis suppressors negatively regulate a broad set of cellular activities pertinent to metastasis, such as tumor cell spreading, dormancy, angiogenesis and survival in new microenvironments (Bodenstine and Welch 2008). Like tumor suppressors, expression of metastasis suppressors is often reduced in metastatic cells as compared to non-metastatic counterparts. One such metastasis suppressor is the missing in metastasis (MIM; also known as metastasis suppressor 1 [MTSS1]) gene, expression of which is frequently silent in a subset of metastatic cell lines originating from bladder, breast and prostate cancers (Lee et al 2002, Loberg et al 2005, Nixdorf et al 2004, Parr and Jiang 2009). Recent studies with human cancers have revealed that the loss of MIM expression occurs in 69% of advanced bladder cancers (Wang et al 2007) and 88% of metastatic gastric cancers (Liu et al 2010). Also, MIM expression is considerably upregulated by TBX5, a newly identified tumor suppressor in colon cancers (Yu et al 2010). In breast and gastric cancers, low levels of MIM expression correlate with poor prognosis and may have predictive value for the disease-free survival (Liu et al 2010, Parr and Jiang 2009). However, evidence supporting a pathological role of MIM in tumorigenesis remains fragmentary and sometimes controversial. For example, overexpression of MIM and amplification of the human MIM locus at human chromosome 8q24.1 was found in hepatocellular carcinomas and ovarian carcinomas, respectively (Ma et al 2007, Nowee et al 2007), and increased MIM immunoreactivity was associated with advanced colorectal cancers (Wang et al 2011). MIM was also identified as a Sonic hedgehog responsive gene (Callahan et al 2004), a signaling pathway normally implicated in tumorigenesis (Bailey et al 2007). In this study, we characterized a MIM knockout (KO) mouse strain and observed a defect in the motility of MIM depleted B cells in response to a splenic chemokine and efficient recruitment to the spleen. Furthermore, the aging MIM KO mice have a predisposition to the formation of B-cell lymphoma. Our data suggests that MIM plays a unique role in the development and function of B lymphocytes, and MIM depletion may promote lymphomagenesis through eliciting aberrant interactions between B lineage cells and their microenvironment.

Results and Discussion

We have recently generated a complete MIM knockout mouse strain using a gene trapping vector (Dan Yu 2011). MIM(−/−) mice developed normally and were fertile, but the survival rate of MIM(−/−) mice was significantly lower than that of wild type mice. The majority of the homozygous knockout animals died between 14 to 24 months, and heterozygous mice also died slightly earlier than wild type animals (Fig. 1A). Biopsies of many sick or moribund old animals revealed that they had developed abnormal tissue structures (Table 1). Notably, 81% of the animals had enlarged spleens (Table 1, Fig. S1A), which were also seen in young mice at the ages between 4 to 8 weeks (Fig. 1B). The splenomegly was not due to a possible increase in their sizes because the body weight of MIM(−/−) mice was apparently normal at young (Fig. 1C) or old ages (data not shown). In addition to enlarged spleens, 56% of the aged animals also exhibited hepatomegaly with rough liver surfaces (Table 1, Fig. S1B), although hepatomegaly was not observed in young mice. Also, about 70% MIM(−/−) mice developed enlarged lymph nodes or spleens infiltrated by abnormal lymphoid cells with vesicular nuclei, abundant cytoplasm and small nucleoli (Fig. 2A), a morphology that was distinct from normal lymphocytes in lymph nodes or spleen (Fig. 2C and D), and was consistent with murine diffuse large B lymphoma according to Bethesda classifications (Morse et al 2002). The majority of the infiltrating cells expressed CD20 (Fig. 2B and Fig. S2A) or B220 (Fig. S2B), but were negative for CD3, a T-cell marker (data not shown). The tumor cells expressed CD19 (B-cell marker) and CD5 (expressed in naïve and memory B lymphomas) (Fig. S3A), indicating that they were derived from CD5+ B-cells. To determine the monoclonal nature associated with malignant lymphomas, the tumors harvested from

three MIM(−/−) mice were analyzed by PCR for the VDJ rearrangement of immunoglobulin (Ig) heavy chain genes. As shown in Fig. S3B, the genomic DNA from a wild type spleen yielded three prominent PCR products of 1.3, 1.0 and 0.7 kb, corresponding to DJ_H1, DJ_H2 and DJ_H3 Ig gene rearrangements, respectively (Chang et al 1992). Another expected band of 0.12 kb corresponding to DJ_H4 was barely detectable, presumably due to low resolution in the agarose gel. However, the DNAs of three lymphomas generated only one dominant PCR product, which migrated at the position of DJ_H3, indicating that these tumors were monoclonal. Some aged MIM(−/−) mice also displayed infiltrated leukocytes in the liver and the kidney (Table 1), which contained a mixture of small T- and B-cells (Fig. S2E and F).

MIM was highly expressed in murine splenic B cells but weakly in splenic T cells (Fig. 3A). Because lymphomas are often associated with aberrant differentiation of B cells (Shaffer et al 2002), we thought that MIM depletion could affect B-cell development in different lymphoid organs. Indeed, about 50% decrease in the percentage of CD19+ B cells in the spleen of MIM(−/−) mice was observed (Fig. 3B and 3C). Conversely, the population of B cells was increased by ~20% in the bone marrow and more significantly in the peripheral blood of MIM(−/−) mice (Fig. 3C). Complete blood count analysis revealed normal ranges of most types of hematopoietic cells in MIM(−/−) mice, although the count of white blood cells in MIM(−/−) mice was evidently higher than that of wild type mice (Table S1). We also analyzed several markers of early B-cell development stages in the bone marrow. While bone marrow of MIM(−/−) mice contained a normal percentage of pre-B1 cells ($CD19^+CD117^+/CD25^-$) (Martensson et al. 2010; Rolink 2004), the percentage of pre-B2 cells ($CD19^+/CD117^-/CD25^+$) was 35% higher than that of the wild type mice (Fig. 4A). The population of B cells expressing s-IgM was also reduced by 22% in the bone marrow (Fig. 4A and B) and by 73% in the spleens (Fig. 4B) of MIM(−/−) mice. The percentage of B cells with s-IgD, the marker for a relatively more mature form of naïve B cells, was also significantly decreased in the MIM depleted spleens (Fig. 4C). The reduction of B-cell populations could be caused by replacement of normal B cells with tumor cells. However, we found no apparent tumor-like cells in either the bone marrow or the blood of young mice, suggesting that reduced B cells likely reflected an aberrant B-cell differentiation or altered affinity for different lymphoid organs in MIM deficient mice.

B-cell development is guided by a series of interactions between B lineage cells and a variety of cytokines or chemokines released from stromal cells in the bone marrow and lymphoid organs (LeBien and Tedder 2008). We therefore examined the response of naïve splenic B cells to CXCL13, a primary B-cell chemokine normally released from splenic stromal cells. In Transwell chambers, wild type B cells had nearly 5-fold higher directional migration towards the CXCL13-containing chamber. Yet, MIM(−/−) B cells failed to do so under the same conditions (Fig. 4D and E) even though they expressed a normal level of CXCR5, the receptor for CXCL13, (Fig. S4). It was also possible that the impaired motility response was caused by the targeting vector used in the generation of this mouse strain (Dan Yu 2011). Yet, the heterozygous B cells, which contained a single copy of the targeting vector, migrated slightly slower than wild type cells, the difference was not statistically significant (Fig. 4F).

We have recently observed that MIM depleted embryonic fibroblasts were less polarized and partially impaired in the receptor-mediated endocytosis (Dan Yu 2011). To examine whether MIM depletion also affects B-cell shape changes, we inspected splenic B cells in response to CXCL13 by phase microscopy. While nearly 57% of wild type B cells were markedly polarized upon CXCL13 treatment, the majority of MIM(−/−) B cells retained their rounded morphology (Fig. S5). We also examined endocytosis of CXCR5 and found that MIM(−/−) B cells failed to internalize the receptor after exposed to CXCL13 for 20 min

(Fig. S4). These data suggest that MIM is required for B cells to respond to chemokines by modulation of cell shapes and endocytosis, and that MIM depletion may impair B-cell development by evoking an aberrant communication between B cells and stromal cells.

To determine whether MIM plays a role in human B cells, we analyzed the expression of MIM and other I-BAR domain family members (Abba, IRSp53, IRTKS and FLJ22582) in a series of hematopoietic cells from healthy adult blood donors, including B cells, T cells, monocytes and granulocytes (Fig. 5A). While the transcripts of all other I-BAR domain genes were nearly undetectable, MIM transcripts were readily identified in primary B cells but much less prominent in monocytes, T cells and granulocytes. Compared to T cells, the level of MIM expression in B cells was about 16-fold higher, a result that agrees with the study with mouse samples (Fig. 3A), suggesting that MIM in B cells has a unique function. Next, we analyzed 11 human B acute lymphocytic leukemia (B-ALL) cases and detected the majority (73%) of the samples contained low levels of MIM expression (Fig. 5B). Furthermore, there were negligible amounts of MIM transcripts in nine B-ALL cell lines (Fig. 5B). In screening of seven human and one murine B lymphoma cell lines, we only detected a weak level of MIM protein in SU-DHL-6 B-cells (Fig. 5C). We also failed to detect abundant MIM protein in a B-cell lymphoma from a patient (Fig. S6, lane a). Thus, low or absent MIM expression is common in these B-cell malignancies.

The mammalian MIM gene encodes a protein product containing an N-terminal region of 250 amino acids that is structurally similar to that of IRSp53 and distantly related to Bin-Amphiphysin-Rvs (BAR) domain, a motif that is present in a series of membrane modeling proteins (Frost et al 2009, Gallop and McMahon 2005). Because the BAR domains of MIM and IRSp53 have a unique zeppelin-like structure with the membrane binding surface on the convex face (Lee et al 2007, Millard et al 2005, Scita et al 2008), they have been recently used to define a subfamily of the BAR domain proteins as inverse BAR (I-BAR) domain family, including MIM, Abba, IRSp53, IRTKS and FLJ22582. In vitro studies have documented the role of MIM in membrane curvature, which is broadly related to cell migration, endocytosis and cell-substratum interactions (Bompard et al 2005, Lin et al 2005, Mattila et al 2007, Woodings et al 2003). Recent studies with other MIM knockout murine strains also indicated a role of MIM in the intercellular interaction in the kidney cells (Saarikangas et al 2011, Xia et al 2010). Yet, the role of MIM in the modulation of cell migration appears to be complex. We had previously shown that overexpression of a MIM construct inhibited cell migration in response to extracellular stimuli (Lin et al 2005). Similarly, suppression of MIM by RNA interference increased the locomotion of breast cancer cells in vitro (Parr and Jiang 2009). On the other hand, a Drosophila mutant with depletion of dMIM expression exhibited a defect in a directional motility of border cells (Quinones and Oro 2010), suggesting that MIM acts differently under physiological conditions. Consistent with this finding, we also observed here a defect in the motility response of MIM(−/−) B-cells to CXCL13, the signaling of which is required for B cells to home to lymphoid follicles in the spleen and Peyer patches and for lymphoid organ development (Lipp and Muller 2004). Inability to respond to CXCL13 may partially explain the increased accumulation of B cells in the peripheral blood and the decrease in the spleens of MIM knockout mice. Since MIM is an intracellular protein and regulates the actin cytoskeleton-mediated membrane dynamics, MIM deficiency may affect signaling pathways of other types of chemokines released from stromal cells in the bone marrow, and thereby possibly influencing B-cell differentiation at an earlier stage such as the transition from pre-B2 to immature B-cells as detected herein. However, we could not rule out completely the possibility that the targeting event in our MIM knockout mice may create these phenotypes through a secondary and unknown mechanism.

Improper interactions of stem cells or progenitors with stromal cells have been associated with cancers including human lymphoma (Egeblad et al 2010, Gribben 2010, Mahadevan et al 2005) and murine lymphoma (Middendorp et al 2009). Furthermore, upregulated chemokine signaling pathways are thought to promote tumor progression by driving leukocyte infiltration and angiogenesis and by establishing a tumor milieu favoring metastases (Karnoub and Weinberg 2006). Yet, we show here that MIM is necessary for the migration of B cells toward CXCL13, a primary chemokine for B cells, and increased response to chemokines is often associated with metastases (McAllister and Weinberg 2010). It is also paradoxical to observe extensive lymphoid infiltrates in various organs with MIM(−/−) mice. One possibility is that the MIM-mediated response to chemotactic factors is not directly involved in the infiltration of all the leukocytes into peripheral organs and may be limited to specific types of cells in response to specific extracellular cues. Indeed, in one case we found that an infiltrate in the liver of a MIM(−/−) mouse was more dominated by T cells than B cells. It is also interesting to observe MIM(−/−) embryonic fibroblasts, which expressed modest amounts of MIM, had a normal motility in the presence of growth factors but were only impaired under conditions with low percentages of serum (Dan Yu 2011). Thus, it appears that MIM regulates cellular motility differently depending upon microenvironments. This plastic property could provide an advantage to stem cells or progenitors during their transition to malignancies under a pathological condition. For example, reduced MIM expression might impair a normal stem cell-stroma interaction and lead to improper homing of stem cells or progenitor cells to a location which would otherwise protect them from unwanted hazards but release chemotactic signals in which the function of MIM is not necessary. Consequently, this mismatch between progenitor cells and their microenvironment might increase their susceptibility to oncogenic insults and their chances to become cancer initiating cells after accumulation of mutational hits. MIM depletion may affect other signaling pathways implicated in lymphomagenesis. Notably, MIM is implicated in the signaling of Sonic hedgehog, which has been found to play a critical role in the interaction between lymphoma and their immune microenvironment (Dierks et al 2007, Lindemann 2008). Although the exact role of MIM in hedgehog pathways in vivo remains undefined (Liu et al 2011, Saarikangas et al 2011), MIM may act in negative concert with hedgehog proteins in B cells, and MIM depletion may facilitate the response of neoplastic B cells to hedgehogs. In the preparation of this manuscript, Liu has reported that frog MIM protein is associated with Daam1 (Liu et al 2011), a formin family protein that is implicated in the actin polymerization and acts as a signaling factor downstream of Wnt5a. Interestingly, mice with depletion of Wnt5a were also prone to lymphomagenesis (Liang et al 2003), suggesting of an alternative link from MIM depletion to lymphoma progression.

Materials and Methods

Antibodies

Polyclonal MIM antibody was described previously (Lin et al 2005). Anti-CD20 antibody was purchased from Millipore (Billerica, MA); anti-B220, anti-Thy1, anti-CD4 and anti-CD8 antibodies were provided by Dr. David Scott; anti-CD3 antibody from Calbiochem (Gibbstown, NJ); allophycocyanin (APC)-conjugated anti-CD19, phycoerythrin (PE)-conjugated anti-CD25, and fluorescein isothiocyanate (FITC)-conjugated anti-CD117 were from Biolegend (San Diego, CA). FITC-conjugated anti-IgM was from Southern Biotech (Birmingham, AL). PE-conjugated anti-IgD was from eBioscience (San Diego, CA).

Animals

Generation of MIM knockout mice has been described (Yu et al 2011). The knockout mice have been back crossed with C57BL/6 for seven to nine generations to reach a nearly

homogenous genetic background and been bred in the vivarium facility at University of Maryland Baltimore. All the animal experiments were conducted in compliance with protocols instituted by the Institutional Animal Care and Use Committee of the University of Maryland School of Medicine.

Histological analysis

Mice were euthanized at the ages of 14–28 months and examined at necropsy for the presence of tumors. Tumors and tissue organs including spleen, lymph nodes, thymus, lung, liver, femur, kidney, brain, pancreas, intestine, colon, and heart were dissected, fixed and stained with hematoxylin and eosin (HE) as described previously (Wang et al 2007). Sections were examined microscopically and the presence of lymphoma was identified according to the Bethesda classification (Morse et al 2002). To determine the B-cell origin of the lymphomas, sections containing lymphomas were immunostained with anti-CD20, B220 and CD3 antibodies, respectively, as described previously (Wang et al 2007).

Western blot

Splenic B-cells were purified according to the procedure as described previously (Su et al 2008). Briefly, spleens were dissected from animals and minced. The resulting non-adherent cells were collected in B-cell medium (RPMI 1640 medium supplemented with 5% FBS, 2 mM L-glutamine and 50 μM β-mecaptoethanol), and were incubated with anti T-cell mixture (anti-Thy1, anti-CD4 and anti-CD8) for 30 min followed by treatment with Low Tox complement (Cedarlane Laboratories, Burlington, NC) according to the manufacturer's instruction. Purified B cells were lysed in SDS sample buffer and subject to 8% SDS-PAGE followed by immunoblotting using anti-MIM polyclonal antibody (Wang et al 2007). Equal protein loading on gels was confirmed by anti-actin antibody. To isolate human B cells, mononuclear cells were isolated from peripheral blood and incubated with magnetic beads coated with CD19 monoclonal antibody for 3min at 4°C. The magnetic beads were collected, and washed with PBS and further incubated in RPMI1640 medium at 37°C in an atmosphere of 5% CO_2. The magnetic beads were separated from CD19+ B cells by using Dynal MPC device (Dynal Biotech).

A human lymphoma specimen was obtained as a lymph node biopsy from a patient with B-cell lymphoma with informed consent under an IRB approved human subject research protocol.

Flow cytometry

Cells isolated from bone marrow or spleen were incubated with appropriate surface marker antibodies for 40 min at 4°C, washed once with PBS containing 0.5% BSA and analyzed on FACSCalibur flow cytometer (BD Biosciences). Data were analyzed with Flowjo software.

Cell motility assay

B-cell migration was analyzed using Costar Transwell plates with 5-μm pore size (Corning, Lowell, MA). Briefly, 10^6 B-cells suspended in 100 μL of B-cell medium were loaded into the upper chamber of a Transwell plate. The lower chamber was loaded with 600 μL of the same medium containing 1 μg/mL CXCL13. In a different experiment, a range of CXCL13 concentrations from 0 to 1 μg/mL was used. The control sample was set up with the lower chamber containing the medium alone. The plate was incubated at 37°C with constant 5% CO_2 supply. After 2 h of incubation, the upper chambers were removed and the cells that had migrated into the lower chamber were counted with hematocytometer. The percentage of migrated cells was calculated by dividing the number of cells collected in the lower chamber by the total cell number loaded into the plate at the initial set up.

Analysis of the clonality of lymphomas

Genomic DNAs were purified from formaldehyde-fixed tissues with FFPE Tissue Kit (Qiagen, cat# 56404) or from fresh tumors with DNeasy kit (Qiagen, cat# 695060). The purified DNAs were used as the templates in PCR using DSF and JH4 primers specific for mouse DJ DNA arrangement (Chang et al. 1992). DSF primer: 5′-AGGGATCCTTGTGAAGGGATCTACTACTGTG-3′; JH4 primer: 5′-AAAGACCTCCAGAGGCCATTCTTACC-3′. PCRs were carried out using Pfuturbo DNA polymerase (Stratagene) under the condition: 35 cycles of 95°C 30s, 61.5°C 30s, 72°C 1min and followed by 72°C 10min for extension.

Microarray and data analysis

Microarray expression analysis was performed using the Affymetrix GeneChip Human Gene 1.0 ST Array, which contains 764,885 probes representing 28,869 annotated genes. We analyzed a total of 9 B acute lymphoblastic leukemia (B-ALL) cell lines, each repeated three times, 11 primary precursor B-ALL patient samples, 4 samples of primary human peripheral blood CD19+ B cells, 8 samples of primary normal human peripheral blood T cells, 4 samples of primary normal human peripheral blood granulocytes, and 2 samples of primary normal human peripheral blood monocytes. Microarray data analyses were performed using GeneSpring GX software (Agilent Technologies).

Analysis of CXCR5 endocytosis

5×10^6 spleenocytes were incubated in B-cell medium with or without 1 μg/mL CXCL13 at 37°C in 5% CO_2 for 20 min, cells were then placed on ice, washed twice with ice-cold RPMI1640 containing 0.5% BSA and stained at 4°C with APC-CD19 and PE-Cy7-CXCR5 mAbs (R&D Systems), and analyzed by flow cytometry.

Supplementary Material

Refer to Web version on PubMed Central for supplementary material.

References

Bailey JM, Singh PK, Hollingsworth MA. Cancer metastasis facilitated by developmental pathways: Sonic hedgehog, Notch, and bone morphogenic proteins. J Cell Biochem. 2007; 102:829–839. [PubMed: 17914743]

Bodenstine TM, Welch DR. Metastasis suppressors and the tumor microenvironment. Cancer Microenviron. 2008; 1:1–11. [PubMed: 19308680]

Bompard G, Sharp SJ, Freiss G, Machesky LM. Involvement of Rac in actin cytoskeleton rearrangements induced by MIM-B. J Cell Sci. 2005; 118:5393–5403. [PubMed: 16280553]

Callahan CA, Ofstad T, Horng L, Wang JK, Zhen HH, Coulombe PA, et al. MIM/BEG4, a Sonic hedgehog-responsive gene that potentiates Gli-dependent transcription. Genes Dev. 2004; 18:2724–2729. [PubMed: 15545630]

Chang Y, Paige CJ, Wu GE. Enumeration and characterization of DJH structures in mouse fetal liver. EMBO J. 1992; 11:1891–1899. [PubMed: 1582417]

XHZ, Dan Yu; Zhao, Xianfeng Frank; Williams, Mark; Carey, Gregory B.; Smith, Elizabeth; Scott, David; Zhu, Jianwei; Zhan, Xi. Mice deficient in MIM expression are predisposed to tumor formation. 2011

Dierks C, Grbic J, Zirlik K, Beigi R, Englund NP, Guo GR, et al. Essential role of stromally induced hedgehog signaling in B-cell malignancies. Nat Med. 2007; 13:944–951. [PubMed: 17632527]

Egeblad M, Nakasone ES, Werb Z. Tumors as organs: complex tissues that interface with the entire organism. Dev Cell. 2010; 18:884–901. [PubMed: 20627072]

Frost A, Unger VM, De Camilli P. The BAR domain superfamily: membrane-molding macromolecules. Cell. 2009; 137:191–196. [PubMed: 19379681]

Gallop JL, McMahon HT. BAR domains and membrane curvature: bringing your curves to the BAR. Biochem Soc Symp. 2005:223–231. [PubMed: 15649145]

Gribben JG. Implications of the tumor microenvironment on survival and disease response in follicular lymphoma. Curr Opin Oncol. 2010; 22:424–430. [PubMed: 20679770]

Karnoub AE, Weinberg RA. Chemokine networks and breast cancer metastasis. Breast Dis. 2006; 26:75–85. [PubMed: 17473367]

LeBien TW, Tedder TF. B lymphocytes: how they develop and function. Blood. 2008; 112:1570–1580. [PubMed: 18725575]

Lee SH, Kerff F, Chereau D, Ferron F, Klug A, Dominguez R. Structural basis for the actin-binding function of missing-in-metastasis. Structure. 2007; 15:145–155. [PubMed: 17292833]

Lee YG, Macoska JA, Korenchuk S, Pienta KJ. MIM, a potential metastasis suppressor gene in bladder cancer. Neoplasia. 2002; 4:291–294. [PubMed: 12082544]

Liang H, Chen Q, Coles AH, Anderson SJ, Pihan G, Bradley A, et al. Wnt5a inhibits B cell proliferation and functions as a tumor suppressor in hematopoietic tissue. Cancer Cell. 2003; 4:349–360. [PubMed: 14667502]

Lin J, Liu J, Wang Y, Zhu J, Zhou K, Smith N, et al. Differential regulation of cortactin and N-WASP-mediated actin polymerization by missing in metastasis (MIM) protein. Oncogene. 2005; 24:2059–2066. [PubMed: 15688017]

Lindemann RK. Stroma-initiated hedgehog signaling takes center stage in B-cell lymphoma. Cancer Res. 2008; 68:961–964. [PubMed: 18281468]

Lipp M, Muller G. Lymphoid organogenesis: getting the green light from RORgamma(t). Nat Immunol. 2004; 5:12–14. [PubMed: 14699400]

Liu K, Wang G, Ding H, Chen Y, Yu G, Wang J. Downregulation of metastasis suppressor 1(MTSS1) is associated with nodal metastasis and poor outcome in Chinese patients with gastric cancer. BMC Cancer. 2010; 10:428. [PubMed: 20712855]

Liu W, Komiya Y, Mezzacappa C, Khadka DK, Runnels L, Habas R. MIM regulates vertebrate neural tube closure. Development. 2011; 138:2035–2047. [PubMed: 21471152]

Loberg RD, Neeley CK, Adam-Day LL, Fridman Y, St John LN, Nixdorf S, et al. Differential expression analysis of MIM (MTSS1) splice variants and a functional role of MIM in prostate cancer cell biology. Int J Oncol. 2005; 26:1699–1705. [PubMed: 15870888]

Ma S, Guan XY, Lee TK, Chan KW. Clinicopathological significance of missing in metastasis B expression in hepatocellular carcinoma. Hum Pathol. 2007; 38:1201–1206. [PubMed: 17442377]

Mahadevan D, Spier C, Della Croce K, Miller S, George B, Riley C, et al. Transcript profiling in peripheral T-cell lymphoma, not otherwise specified, and diffuse large B-cell lymphoma identifies distinct tumor profile signatures. Mol Cancer Ther. 2005; 4:1867–1879. [PubMed: 16373702]

Mattila PK, Pykalainen A, Saarikangas J, Paavilainen VO, Vihinen H, Jokitalo E, et al. Missing-in-metastasis and IRSp53 deform PI(4,5)P2-rich membranes by an inverse BAR domain-like mechanism. J Cell Biol. 2007; 176:953–964. [PubMed: 17371834]

McAllister SS, Weinberg RA. Tumor-host interactions: a far-reaching relationship. J Clin Oncol. 2010; 28:4022–4028. [PubMed: 20644094]

Middendorp S, Xiao Y, Song JY, Peperzak V, Krijger PH, Jacobs H, et al. Mice deficient for CD137 ligand are predisposed to develop germinal center-derived B-cell lymphoma. Blood. 2009; 114:2280–2289. [PubMed: 19608748]

Millard TH, Bompard G, Heung MY, Dafforn TR, Scott DJ, Machesky LM, et al. Structural basis of filopodia formation induced by the IRSp53/MIM homology domain of human IRSp53. EMBO J. 2005; 24:240–250. [PubMed: 15635447]

Morse HC 3rd, Anver MR, Fredrickson TN, Haines DC, Harris AW, Harris NL, et al. Bethesda proposals for classification of lymphoid neoplasms in mice. Blood. 2002; 100:246–258. [PubMed: 12070034]

Nixdorf S, Grimm MO, Loberg R, Marreiros A, Russell PJ, Pienta KJ, et al. Expression and regulation of MIM (Missing In Metastasis), a novel putative metastasis suppressor gene, and MIM-B, in bladder cancer cell lines. Cancer Lett. 2004; 215:209–220. [PubMed: 15488640]

Nowee ME, Snijders AM, Rockx DA, de Wit RM, Kosma VM, Hamalainen K, et al. DNA profiling of primary serous ovarian and fallopian tube carcinomas with array comparative genomic hybridization and multiplex ligation-dependent probe amplification. J Pathol. 2007; 213:46–55. [PubMed: 17668415]

Parr C, Jiang WG. Metastasis suppressor 1 (MTSS1) demonstrates prognostic value and anti-metastatic properties in breast cancer. Eur J Cancer. 2009; 45:1673–1683. [PubMed: 19328678]

Quinones GA, Oro AE. BAR domain competition during directional cellular migration. Cell Cycle. 2010; 9

Saarikangas J, Mattila PK, Varjosalo M, Bovellan M, Hakanen J, Calzada-Wack J, et al. Missing-in-metastasis MIM/MTSS1 promotes actin assembly at intercellular junctions and is required for integrity of kidney epithelia. J Cell Sci. 2011; 124:1245–1255. [PubMed: 21406566]

Scita G, Confalonieri S, Lappalainen P, Suetsugu S. IRSp53: crossing the road of membrane and actin dynamics in the formation of membrane protrusions. Trends Cell Biol. 2008; 18:52–60. [PubMed: 18215522]

Shaffer AL, Rosenwald A, Staudt LM. Lymphoid malignancies: the dark side of B-cell differentiation. Nat Rev Immunol. 2002; 2:920–932. [PubMed: 12461565]

Wang D, Xu MR, Wang T, Li T, Zhu JW. MTSS1 Overexpression Correlates with Poor Prognosis in Colorectal Cancer. J Gastrointest Surg. 2011

Wang Y, Liu J, Smith E, Zhou K, Liao J, Yang GY, et al. Downregulation of missing in metastasis gene (MIM) is associated with the progression of bladder transitional carcinomas. Cancer Invest. 2007; 25:79–86. [PubMed: 17453818]

Woodings JA, Sharp SJ, Machesky LM. MIM-B, a putative metastasis suppressor protein, binds to actin and to protein tyrosine phosphatase delta. Biochem J. 2003; 371:463–471. [PubMed: 12570871]

Xia S, Li X, Johnson T, Seidel C, Wallace DP, Li R. Polycystin-dependent fluid flow sensing targets histone deacetylase 5 to prevent the development of renal cysts. Development. 2010; 137:1075–1084. [PubMed: 20181743]

Yu J, Ma X, Cheung KF, Li X, Tian L, Wang S, et al. Epigenetic inactivation of T-box transcription factor 5, a novel tumor suppressor gene, is associated with colon cancer. Oncogene. 2010; 29:6464–6474. [PubMed: 20802524]

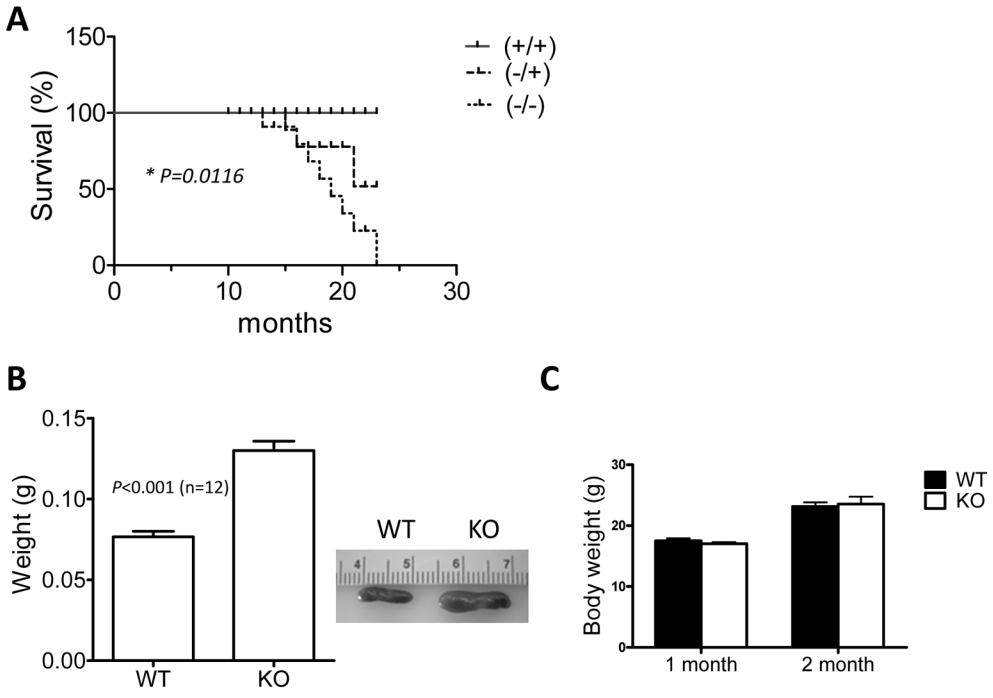

Fig. 1. Phenotypes of MIM KO mice

(A) MIM(−/−) mice have a shorter life span as compared to MIM(+/−) and MIM(+/+) mice as observed within 24 months. The *p* value (*t* test) refers to the difference between MIM(−/−) and MIM(+/+) mice. (B) Comparison of the spleens from a two-month old MIM(−/−) mouse and a MIM(+/+) mouse at the same age based on the weight (right, n=12) and the size (right). (C) Comparison of the whole body weight of MIM(−/−) and MIM(+/+) mice at 1 and 2 month old (n=6), respectively.

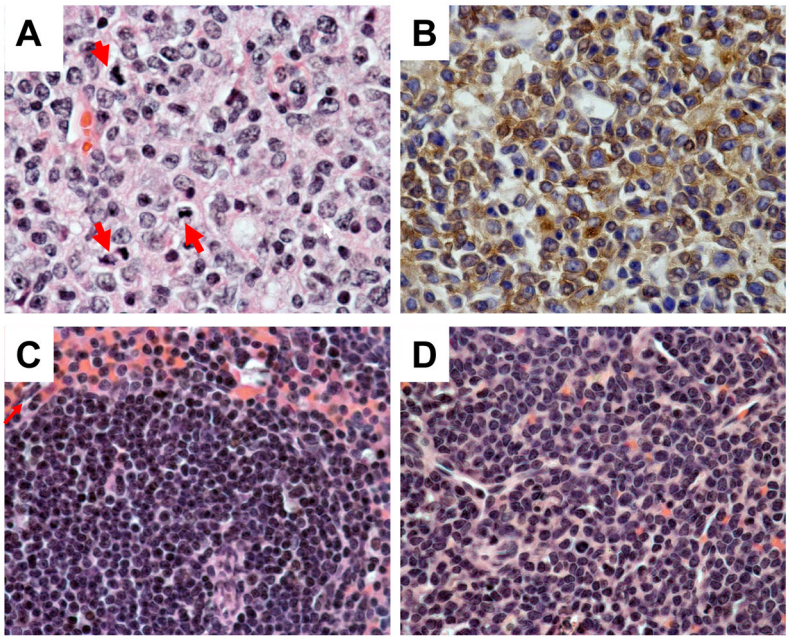

Fig. 2. Histological analysis of lymphoma developed in MIM KO mice

(A) HE staining of a lymphoma section. Several mitotic cells were indicated by arrows. (B) A lymphoma section was stained with CD20 antibody. (C) HE staining of a normal lymph node. (D) HE staining of a normal spleen. Original magnifications: 600 x.

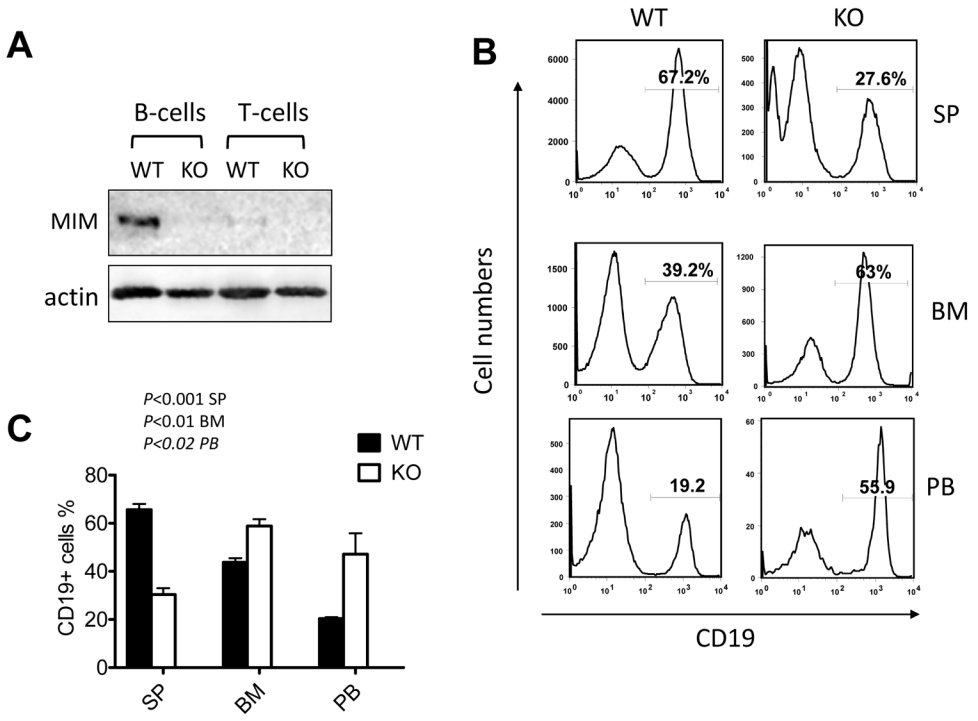

Fig. 3. Aberrant distribution of MIM KO B lineage cells in the bone marrow and the spleen

(A) MIM is abundantly expressed in splenic B cells but weakly in splenic T cells. (B) Flow cytometry analysis of $CD19^+$ B cells isolated from the spleen (SP), the bone marrow (BM) and the peripheral blood (PB). (C) Quantification of $CD19^+$ B cells in lymphoid organs (n=3). *P* values (*t* test) refer to the statistical difference between WT and KO samples.

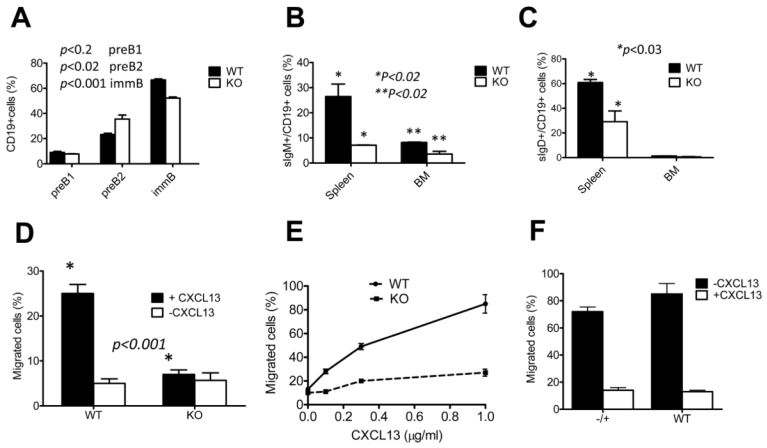

Fig. 4. MIM KO mice were partially impaired in B-cell development and the motility response to CXCL13

(A) The bone marrow of MIM KO mice contained an increased population of pre-B2 cells but a decreased population of immature B cells. (B) MIM KO mice developed significantly less sIgM+ B cells in both spleen and bone marrow. (C) MIM KO mice developed less sIgD + B-cells in the spleen. (D) Splenic MIM KO B cells were unable to migrate efficiently into Transwell chambers containing 1 μg/mL CXCL13. (E) Motility of B cells was measured at difference doses of CXCL13. (F) MIM heterozygous B cells displayed a normal response to CXCL13. All the data represent three independent experiments (mean ± SEM).

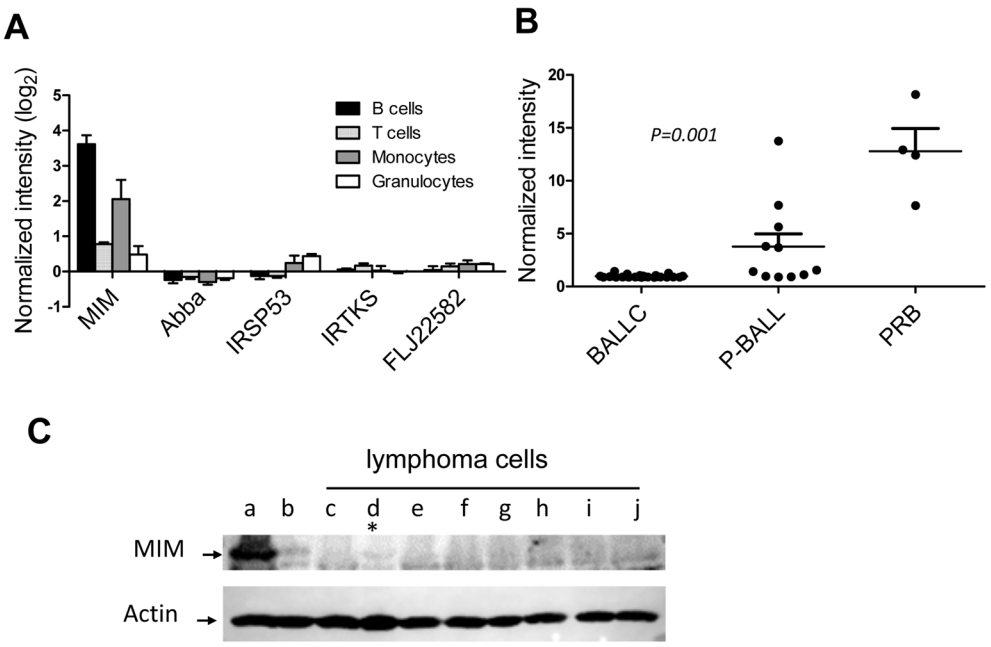

Fig. 5. MIM is abundantly expressed in normal human B cells but poorly expressed in neoplastic B cells

(A) Microarray analysis of the transcripts of the I-BAR domain family members in human primary B cells (n=4), T-cells (n=8), granulocytes (n=4) and monocytes (n=2). (B) Differential expression of MIM in B acute lymphocytic leukemia (BALL) and normal primary peripheral blood B cells. MIM expression was measured by microarray in acute BALL cell lines (n = 9 cell lines, in triplicates, total 27 arrays), precursor B-ALL (P-BALL) patient samples (n=11) and normal peripheral blood CD19+ B cells (PRB) (n=4). (C) MIM is poorly expressed in lymphoma cell lines as measured by Western blot. a, CMK (a MIM expressing human megakaryoblastic cell line); b, MCF-7 breast cancer cells; c, WEHI231 (murine); d, SU-DHL-6; e, SU-DHL-4; f, Ramos; g, RAJI; h, Daudi; i, Karpas-k422; and j, Farage. *, indicating a weak MIM expression.

Table 1

phenotypes of MIM knockout mice

#	Age (months)	Gender	Liver	Spleen	LN	Inflammation *
422	20	F	AN	L	-	+
388	21	M	AN	N	Lm	+
1302	15	F	AN	L	Lm	+
220	21	F	N	L	-	+
82	23	M	AN	L	-	+
244	23	F	N	N	Lm	+
300	26	M	AN	L	Lm	+
203	14	M	N	L	Lm	+
556	22	F	AN	L	Lm	+
277	24	F	N	L	-	+
182	16	M	AN	L	Lm	+
433	21	M	N	L	Lm	+
248	26	F	AN	L	Lm	+
108	23	M	AN	L	Lm	+
1162	16	F	N	L	Lm	+
1170	16	M	N	N	Lm	+
278	16	M	N	N	-	−
1281	14	M	ND	ND	Lm	+

AN, abnormal; L, enlarged; Lm, lymphoma; N, normal; and ND, not determined.

*, inflammation was identified by leukocyte infiltration into organs such as liver and kidney.